http://ansinet.com/itj

ITJ

ISSN 1812-5638

INFORMATION TECHNOLOGY JOURNAL

ANSInet
Asian Network for Scientific Information
308 Lasani Town, Sargodha Road, Faisalabad - Pakistan

Information Technology Journal 13 (18): 2736-2742, 2014
ISSN 1812-5638

ansinet
Asian Network for Scientific Information

RESEARCH ARTICLE OPEN ACCESS

DOI: 10.3923/itj.2014.2736.2742

Temporal Coupled-Mode Theory Analysis and Test Methods Comparison of a K-Band MMIC Bandpass Filter with Dual Orthogonal Resonant Modes

Wei Chen, Xiuqin Xu, Hui Xu, Ming Hong, Zhiyu Wang, Yongheng Shang, Dongdong Liu, Min Zhou, Zhengliang Huang and Faxin Yu
School of Aeronautics and Astronautics, Zhejiang University, Hangzhou, 310027, China

Corresponding Author:
Min Zhou,
School of Aeronautics and Astronautics,
Zhejiang University, Hangzhou, 310027,
China

ABSTRACT

This study presents the temporal Coupled-Mode Theory (CMT) analysis of a K-band MMIC (Microwave Monolithic Integrated Circuit) bandpass filter with dual orthogonal resonant modes. Two test methods are applied and compared in the filter response measurement. The dimensions of the MMIC filter, whose chip size is 1.9×1.35 mm, are optimized based on the FEM (Finite Element Method) simulation assisted temporal coupled-mode theory. As a two-port reciprocal system, the transmission and reflection responses of the filter are deduced. GaAs MMIC IPD (Integrated Passive Device) technology is applied for chip fabrication. The test results using a probe station fit well with the simulation results. A testing fixture is introduced to model the practical application scenario, whose measurement results, after de-embedment, have shown consistency with the simulation and the probe station test results.

Key words: Bandpass filter, coupled mode theory, dual orthogonal resonant mode, GaAs MMIC IPD technology

INTRODUCTION

Microstrip bandpass filters are essential high frequency components in microwave communication systems. Microstrip bandpass filters with improved performance for out-of-band and in-band responses, reduced size, high rejection and low insertion loss are widely required in modern microwave communication system (Matthaei *et al*., 1980; Hong and Lancaster, 2001). With the improvement of design and process technology, using MMIC technology to realize microwave filters has shown great advantages (Delmond *et al*., 1995) and attracted many researchers. For example, Vindevoghel and Descamps (2000) has designed the K-band narrowband active GaAs MMIC filters with central frequency at 22 GHz and a bandwidth of 0.75 GHz. A fixed-frequency and a tunable K-band active bandpass filter has been proposed (Fan *et al*., 2005), the operation frequency of the fix-frequency filter centered at 22.6 GHz with the working bandwidth of 900 MHz. Furthermore, based on MMIC technology, several microstrip dual-mode filters are introduced for applications in communication system (Lee *et al*., 2000; Zhang *et al*., 2008; Liao *et al*., 2007). In order to achieve the properties of high compact size, low insertion loss, high selectivity, harmonic suppression, extended stopped band, more rigorous microstrip bandpass filters are designed (Wei *et al*., 2011; Wang and Guan, 2012; Xu *et al*., 2013; Wolff, 1972; Hong *et al*., 2007). Comparing to other filters fabricated by LTCC (Rambabu and Bornemann, 2005) and thin-film technology, the potentially great performance-to-size ratio and the compatibility of such networks with other MMIC circuits by using GaAs MMIC IPD technology can be obtained which are crucial factors in communication system.

In this study, based on the GaAs MMIC IPD technology, an MMIC bandpass filter with dual orthogonal resonant modes are provided and optimized for K-band applications. The temporal coupled-mode theory (Suh *et al*., 2004; Matsunaga, 2003; Lopetegi *et al*., 2002; Krage and Haddad, 1970; Watanabe and Yasumoto, 2000) assisted by FEM simulations is applied for the optimization. The transmission and reflection responses of the filter are measured through two different test methods, direct measurement on probe station and indirect measurement via testing fixture. For the latter case, which models the practical application scenario, de-embedment technique is introduced to retrieve the responses of the filter.

METHODOLOGY

The presented filter A is shown in Fig. 1, whose topological pattern is borrowed from Zhang *et al.* (2008). There are four layers in total. The top layer is a 4.8 μm thick gold layer which contains the pattern of the present bandpass filter. The bottom layer is another gold layer which is used as the ground layer. Between these two layers there are two dielectric layers. The 0.1 mm thick GaAs layer, whose relative dielectric constant is equal to 12.9, is used as the substrate and between the top layer and the GaAs layer locates a thin SiN passivation layer. The SiN layer is an optional layer which is used to protect the electric properties of the GaAs layer.

There are dual orthogonal modes excited in this filter, an odd mode and an even mode, illustrated in Fig. 1. The solid black line indicates the path of direct coupling, the long dashed red line indicates the odd resonant mode and the short dashed blue line indicates the even resonant mode. The length of microstrip along each trace is about the half wavelength at the resonant frequency of each mode. The direct coupling from one feed line to the other is introduced to form an additional transmission zero in the upper stopband. As a result, a bandpass filter with extended upper stopband is achieved.

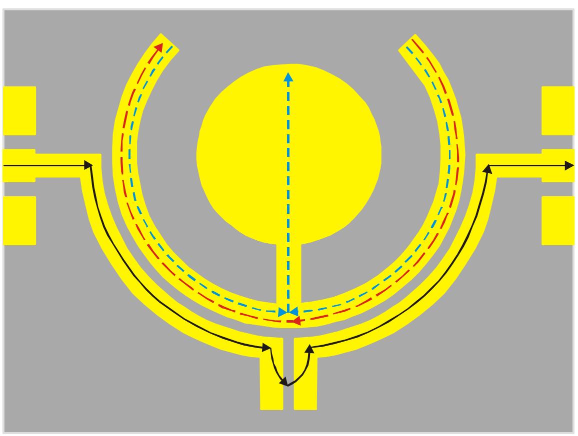

Fig. 1: Illustration of the direct coupling path (solid black line), the odd (long dashed red line) and even (short dashed blue line) resonant modes in the filter

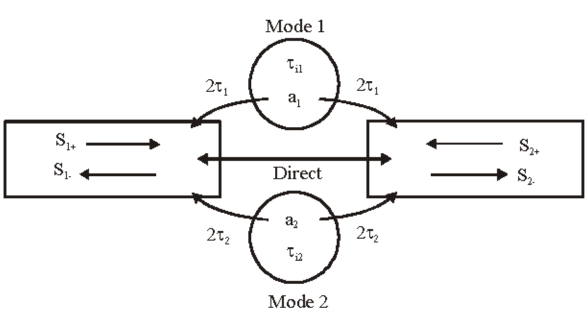

Fig. 2: Simple schematic diagram showing the multi-coupling features of the filter with dual orthogonal resonant modes

As a spatially symmetric (common case) microstrip filter with two orthogonal resonant modes, the coupling schematic is presented in Fig. 2. The incoming wave will propagate along three paths, including two coupling paths via the two resonant modes, respectively and the direct coupling path from one feed line to the other. At the same time, the amplitude of each mode can also decay into the two feed lines. For such a reciprocal filter system, considering the radiation/Ohm loss of the microstrip and the contribution of the direct coupling and assuming the frequency of the odd resonant mode ω_1 is lower than the even resonant mode ω_2 in order to obtain the upper stopband, the dynamic equations of CMT in (Suh *et al.*, 2004) can be rewritten as:

$$\begin{bmatrix} j\omega - j\omega_1 + 1/\tau_1 + 1/\tau_{i1} & 0 \\ 0 & j\omega - j\omega_2 + 1/\tau_2 + 1/\tau_{i2} \end{bmatrix} \begin{pmatrix} a_1 \\ a_2 \end{pmatrix} = e^{-j\omega t'/2} \begin{bmatrix} \sqrt{(-r_d + jt_d)/\tau_1} & -\sqrt{(-r_d + jt_d)/\tau_1} \\ \sqrt{(-r_d - jt_d)/\tau_2} & +\sqrt{(-r_d - jt_d)/\tau_2} \end{bmatrix} \begin{pmatrix} s_{1+} \\ s_{2+} \end{pmatrix} \tag{1}$$

$$\begin{pmatrix} s_{1-} \\ s_{2-} \end{pmatrix} = e^{-j\omega t'} \begin{bmatrix} r_d & jt_d \\ jt_d & r_d \end{bmatrix} \begin{pmatrix} s_{1+} \\ s_{2+} \end{pmatrix} + \begin{bmatrix} \sqrt{(-r_d + jt_d)/\tau_1} & \sqrt{(-r_d - jt_d)/\tau_2} \\ -\sqrt{(-r_d + jt_d)/\tau_1} & \sqrt{(-r_d - jt_d)/\tau_2} \end{bmatrix} \begin{pmatrix} a_1 \\ a_2 \end{pmatrix} \tag{2}$$

where, a_n denotes the amplitude of mode n, ω_n denotes the resonant frequency of mode n, τ_n and τ_{in} denote the lifetimes of mode n due to the coupling to the two feed lines and the radiation/Ohm losses, respectively, s_{m+} and s_{m-} denote the amplitudes of the incoming wave and outgoing wave refer to terminal m, respectively, r_d and jt_d denote the reflection and transmission coefficients of the direct coupling, t' denotes the time delay of the feed line.

The total reflection and transmission of the filter system are deducted from Eq. 1 and 2 as:

$$r = \frac{s_{1-}}{s_{1+}} = [r_d - \frac{(r_d - jt_d)/\tau_1}{j\omega - j\omega_1 + 1/\tau_1 + 1/\tau_{i1}} - \frac{(r_d + jt_d)/\tau_2}{j\omega - j\omega_2 + 1/\tau_2 + 1/\tau_{i2}}]e^{-j\omega t'} \tag{3}$$

$$t = \frac{s_{2-}}{s_{1+}} = [jt_d - \frac{(r_d + jt_d)/\tau_1}{j\omega - j\omega_1 + 1/\tau_1 + 1/\tau_{i1}} - \frac{(-r_d + jt_d)/\tau_2}{j\omega - j\omega_2 + 1/\tau_2 + 1/\tau_{i2}}]e^{-j\omega t'} \tag{4}$$

RESULTS

To achieve a K-band bandpass filter with extended upper stopband, the parameters in Eq. 3 and 4 are optimized as: r_d = 0.97, t_d = 0.075, l/c' = 0.0235 ns, $\omega_1/2\pi$ = 21.62 GHz, $\omega_2/2\pi$ = 22.99 GHz, τ_1 = 0.14 ns, τ_2 = 0.35 ns, τ_{i1} = 1.8 ns, τ_{i2} = 1.9 ns. The dimensions of the filter pattern are then optimized through the software Ansoft HFSS (High Frequency Structure Software). Eigenmode simulation is applied to approach the above parameters. The optimized dimensions of the designed filter are shown in Fig. 3, where, R_1 = 0.285 mm, R_2 = 0.475 mm, R_3 = 0.585 mm, W_1 = 0.07 mm, W_2 = 0.065 mm, L = 0.22 mm, D = 0.04 mm, θ = 44 deg.

The simulated magnitude and phase responses of the optimized filter are illustrated in Fig. 4.

As is shown in Fig. 4, the insertion loss of the proposed filter is less than 1.1 dB at its center frequency. In the whole passband, from 21.86-22.64 GHz, the insertion loss is less than 1.6 dB and the return loss is more than 20 dB. As illustrated in Fig. 4, good linearity is achieved from the transmission phase during the working band. The fabricated MMIC of the filter based on GaAs MMIC IPD technology is showed in Fig. 5. The size of the proposed filter is 1.9×1.35×0.1 mm.

The transmission and reflection responses of the filter are measured through two different test methods, direct measurement on probe station and indirect measurement via testing fixture. With the help of a vector network analyzer (Rohde and Schwarz, ZVA 40), a microwave probe station (Cascade Microtech, Summit 11000 M) and a testing fixture are applied to evaluate the proposed filter, respectively. The probe station provides the direct test results which are close to the simulation results and the measurement via a testing fixture models the real behavior of the filter applied in a T/R module. The testing setup is showed in Fig. 6. The ACP-40-A GSG150 probe is applied in the testing using a probe station.

The measured results through the above two test methods are shown in Fig. 7. The 210 degree phase shifting is applied 1.6 dB insertion loss at 22.25 GHz, less than 2.3 dB insertion loss and more than 20 dB return loss within the whole passband, from 21.86-22.64 GHz. Comparing with the simulation results in Fig. 4, the passband insertion loss has

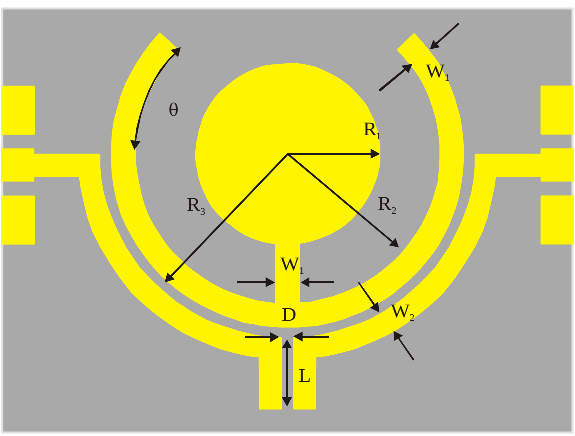

Fig. 3: Dimensions of the filter

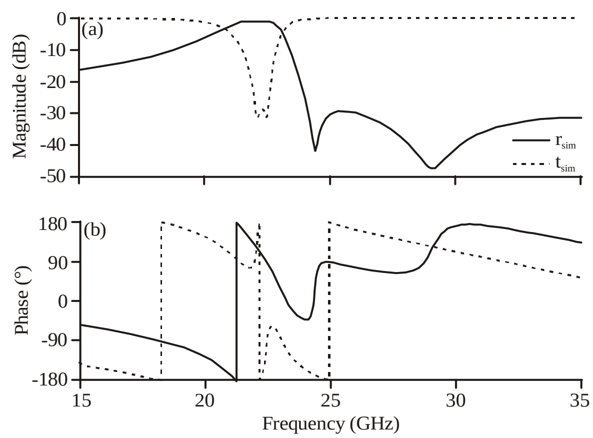

Fig. 4(a-b): Simulation results, (a) Magnitude response of the filter and (b) Phase response of the filter

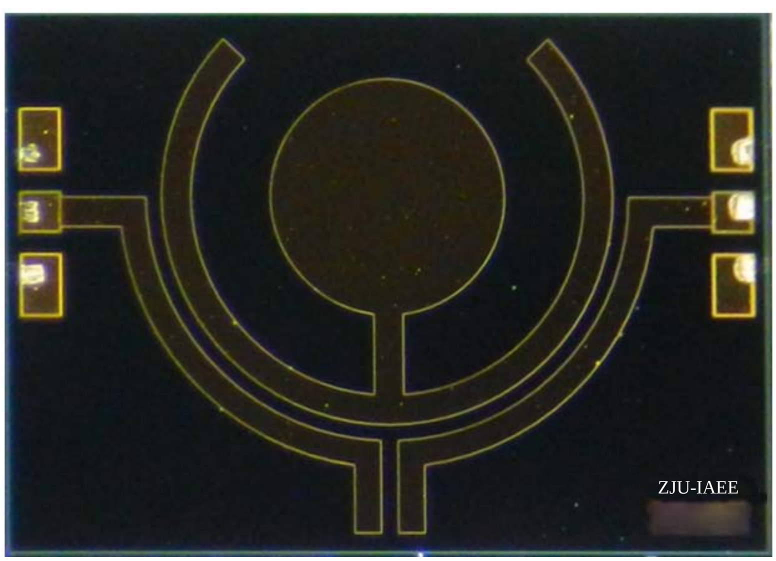

Fig. 5: Fabricated filter based on GaAs MMIC IPD technology

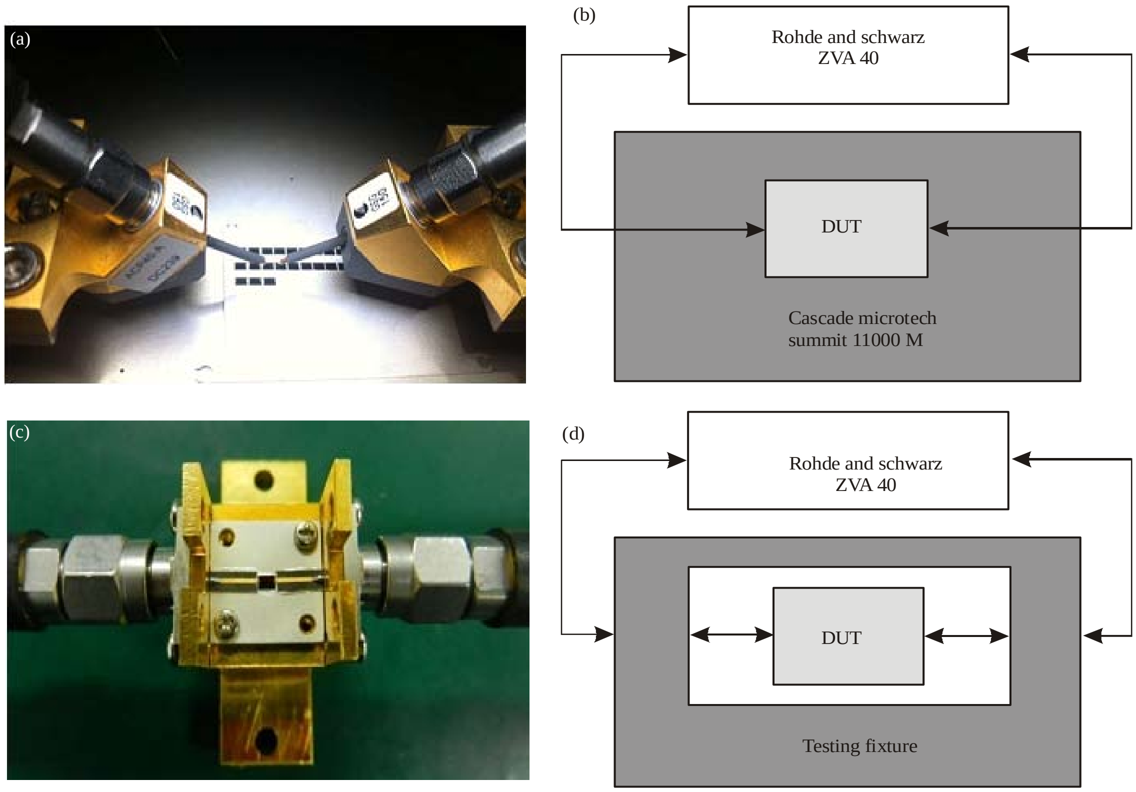

Fig. 6(a-d): (a) Photo, (b) Schematic of the testing setup using a probe station, (c) Photo and (d) Schematic of the testing setup with a testing fixture

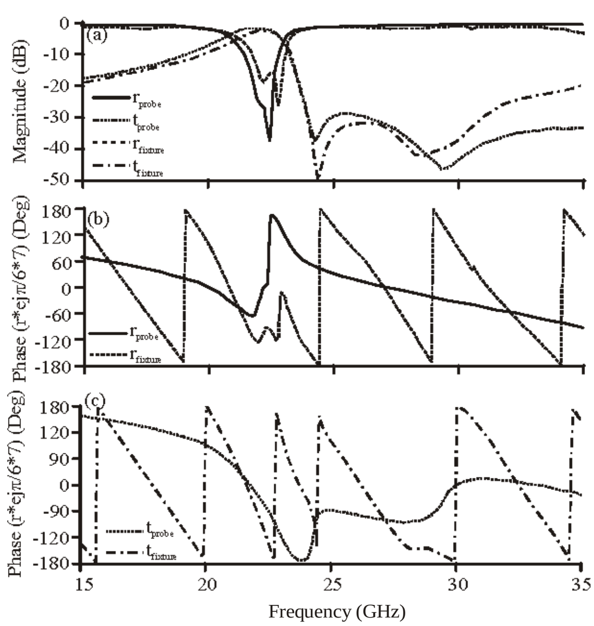

Fig. 7(a-c): Measured results of the MMIC using a probe station (solid blue, dotted green) and the MMIC with a testing fixture (dashed red, dash-dot orange), (a) Magnitude responses, (b) Phase of reflection responses and (c) Phase of transmission responses

increased by 0.5 dB. The main reason for the difference of the insertion loss is due to the processing inaccuracy and the loss in the testing system.

In order to model the real application scenario, a testing fixture is applied to test the proposed filter. The texting fixture is shown in Fig. 6c. Figure 7 illustrates the test results. Results show that the proposed filter has about 2.9 dB insertion loss at 22.25 GHz, less than 3.3 dB insertion loss and more than 20 dB return loss within the whole passband. Comparing with the test results with probe station, more loss and large phase shifting exist. The reason of such difference is due to the mismatching between the MMIC and the testing fixture and the limited accuracy of the applied assembly technology. To fix such difference, de-embedment technique is introduced to retrieve the responses of the filter. The schematic diagram of the de-embedment of the MMIC measurement with a testing fixture is shown in Fig. 8.

Components to be de-embedded on one side of the MMIC in the testing fixture are shown in Fig. 8a. On the other side of the MMIC, same components can be found with mirror symmetry. In order to de-embed the effect of the testing fixture, S-parameter of the components on each side is simulated and output as an S2P file. Substitute the S2P file into the "de-embed components" in the commercial circuit simulation software ADS (Advanced Design Systems), the response of the MMIC can be retrieved from the test results with the testing fixture through the process in Fig. 8b. The de-embedded results are shown in Fig. 9. Results show

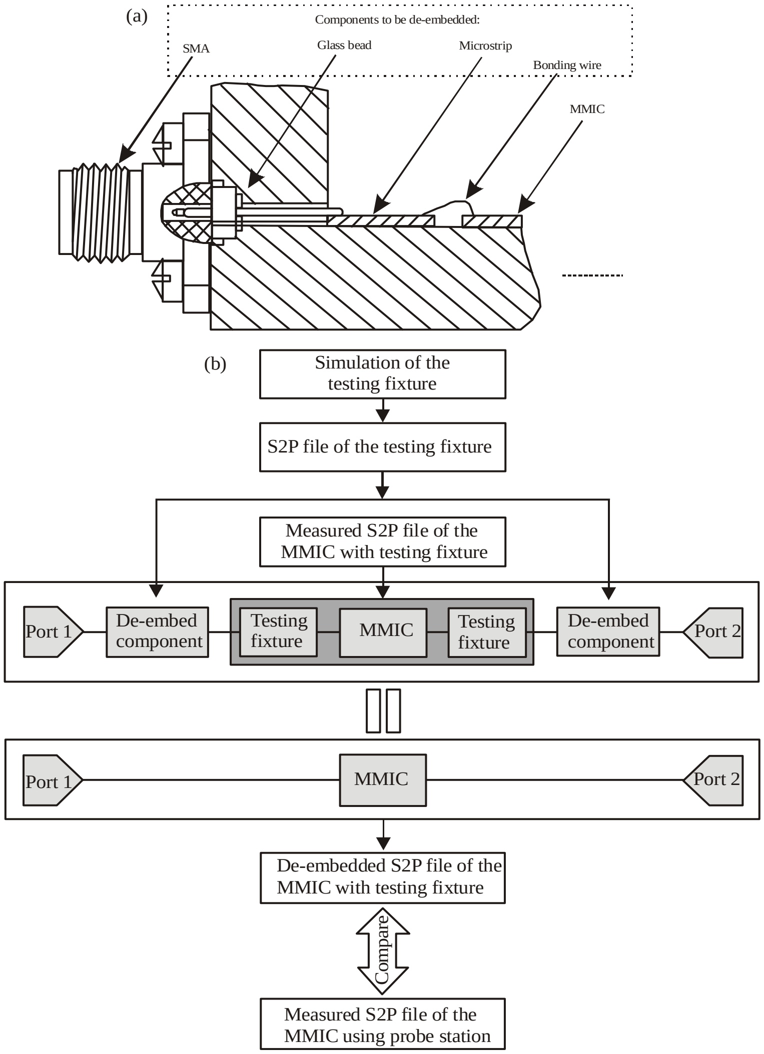

Fig. 8(a-b): (a) Components to be de-embedded on one side of the MMIC in the testing fixture and (b) Schematic diagram of the de-embedment of the MMIC measurement with a testing fixture

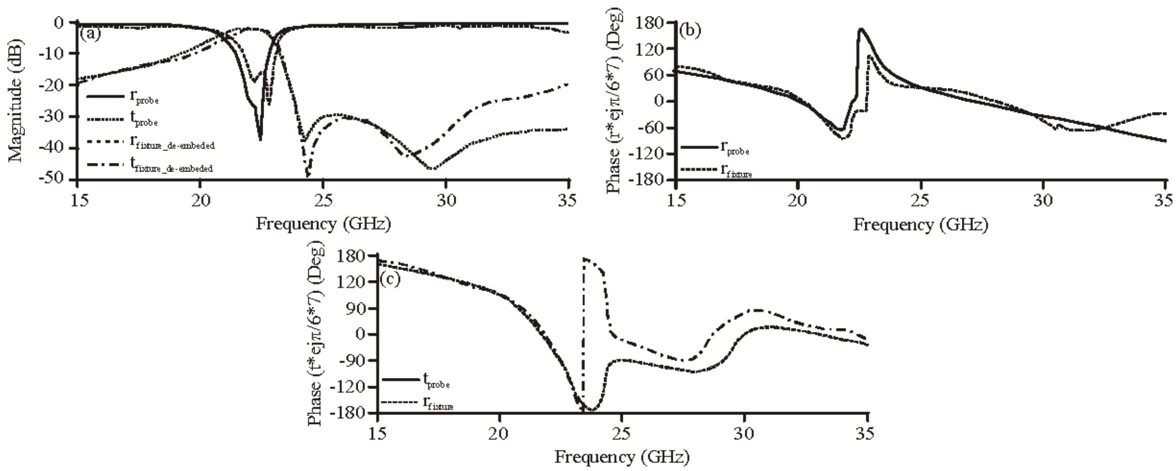

Fig. 9(a-c): Measured results of the MMIC using probe station (solid blue, dotted green) and the de-embedded results of the MMIC with a testing fixture (dashed red, dash-dot orange), (a) Magnitude responses, (b) Phase of reflection responses and (c) Phase of transmission responses

Table 1: Method comparison

	Methods	
Parameters	Network-based filter synthesis method (Rambabu and Bornemann, 2005)	Proposed CMT method in this study
Loss consideration	None	Yes
Design accuracy	Modest	High
Time consumption	Modest	Low

consistency with the simulation and the test results using probe station. Differences between the results through the two test methods are due to the imperfect modeling of the testing fixture.

DISCUSSION

The present CMT analysis method is based on the energy conservation in the multi-resonator filter system. Comparing with the conventional network-based filter synthesis method (Wei *et al.*, 2011; Wang and Guan, 2012; Xu *et al.*, 2013; Wolff, 1972; Hong *et al.*, 2007) our CMT analysis method directly provides the decay rates of each resonant mode, which is more convenient to link with the quality factors obtained directly through eigenmode simulations. When we start to optimize the concrete microstrip filter which contains multi resonant modes through eigenmode simulations, the present method is more direct and less time consuming. Also, our method conveniently includes the dissipations, while most of the published approaches haven't taken the effect of loss into account, thus our approach may save time in fine tuning the filter. The method comparison is shown in Table 1.

CONCLUSION

In conclusion, a K-band MMIC dual-mode bandpass filter with extended upper stopband has been proposed. Based on the temporal coupled-mode theory for a symmetric reciprocal structure system, a FEM simulation assisted optimization is applied to achieve the dimensions of the filter. The transmission and reflection responses of the filter are measured through two different test methods, direct measurement on probe station and indirect measurement via testing fixture. For the latter case, which models the practical application scenario, de-embedment technique is introduced to retrieve the responses of the filter. The de-embedded results have shown consistency with the simulation and the probe station test results. The provided analysis method and test procedure can be easily adapted for dual-mode MMIC bandpass filter designs.

ACKNOWLEDGMENT

This study was supported by the National Science Foundation of China under Grant 61401395 and the Fundamental Research Funds for the Central Universities under Grant 2014QNA4033.

REFERENCES

Delmond, M., L. Billonnet, B. Jarry and P. Guillon, 1995. Microwave tunable active filter design in MMIC technology using recursive concepts. Proceedings of the Microwave and Millimeter-Wave Monolithic Circuits Symposium, May 15-16, 1995, Orlando, FL., USA., pp: 105-108.

Fan, K.W., C.C. Weng, Z.M. Tsai, H. Wang and S.K. Jeng, 2005. K-band MMIC active band-pass filters. IEEE Microwave Wireless Compon. Lett., 15: 19-21.

Hong, J.S. and M.J. Lancaster, 2001. Microstrip Filters for RF/Microwave Applications. 1st Edn., John Wiley and Sons, New York, USA., ISBN-13: 9780471388777, Pages: 488.

Hong, J.S., H. Shaman and Y.H. Chun, 2007. Dual-mode microstrip open-loop resonators and filters. IEEE Trans. Microwave Theory Tech., 55: 1764-1770.

Krage, M.K. and G.I. Haddad, 1970. Characteristics of coupled microstrip transmission lines-I: Coupled-mode formulation of inhomogeneous lines. IEEE Trans. Microwave Theory Tech., 18: 217-222.

Lee, J.R., J.H. Cho and S.W. Yun, 2000. New compact bandpass filter using microstrip/spl lambda//4 resonators with open stub inverter. IEEE Microwave Guided Wave Lett., 10: 526-527.

Liao, C.K., P.L. Chi and C.Y. Chang, 2007. Microstrip realization of generalized Chebyshev filters with box-like coupling schemes. IEEE Trans. Microwave Theory Tech., 55: 147-153.

Lopetegi, T., M.A. Laso, M.J. Erro, M. Sorolla and M. Thumm, 2002. Analysis and design of periodic structures for microstrip lines by using the coupled mode theory. IEEE Microwave Wireless Compon. Lett., 12: 441-443.

Matsunaga, M., 2003. A coupled-mode theory-based analysis of coupled microstrip lines on a ferrite substrate. Prog. Electromagn. Res., 42: 219-232.

Matthaei, G.L., L. Young and E.M.T. Jones, 1980. Microwave Filters, Impedance-Matching Networks and Coupling Structures. Artech House, Norwood, MA., USA., ISBN-13: 978-0890060995, Pages: 1096.

Rambabu, K. and J. Bornemann, 2005. Simplified analysis technique for the initial design of LTCC filters with all-capacitive coupling. IEEE Trans. Microwave Theory Tech., 53: 1787-1791.

Suh, W., Z. Wang and S. Fan, 2004. Temporal coupled-mode theory and the presence of non-orthogonal modes in lossless multimode cavities. IEEE J. Quantum Electron., 40: 1511-1518.

Vindevoghel, J. and P. Descamps, 2000. Narrowband active GaAs MMIC filters n K-band. Proceedings of the 30th European Microwave Conference, October 2-6, 2000, Paris, France, pp: 147-150.

Wang, L. and B.R. Guan, 2012. A novel high selectivity dual-band band-pass filter with inductive source-load coupling. J. Electromagn. Waves Applic., 26: 1734-1740.

Watanabe, K. and K. Yasumoto, 2000. Coupled-mode analysis of coupled microstrip transmission lines using a singular perturbation technique. Prog. Electromagn. Res., 25: 95-110.

Wei, C.L., B.F. Jia, Z.J. Zhu and M. Tang, 2011. Design of different selectivity dual-mode filters with E-shaped resonator. Prog. Electromagn. Res., 116: 517-532.

Wolff, I., 1972. Microstrip bandpass filter using degenerate modes of a microstrip ring resonator. Electron. Lett., 8: 302-303.

Xu, J., W. Wu and C. Miao, 2013. Compact and sharp skirts microstrip dual-mode dual-band bandpass filter using a single Quadruple-Mode Resonator (QMR). IEEE Trans. Microwave Theory Tech., 61: 1104-1113.

Zhang, X.C., Z.Y. Yu and J. Xu, 2008. Design of microstrip dual-mode filters based on source-load coupling. IEEE Microwave Wireless Compon. Lett., 18: 677-679.